arXiv:0904.3560v3 [hep-ph] 3 Aug 2010

Higgs Production and Decay From String Balls vs Black Holes at LHC

Gouranga C. Nayak[1,*]

[1] *Department of Physics, University of Arizona, Tucson, AZ 85721 USA*

Abstract

We study Higgs production and decay from TeV scale string balls and black holes in pp collisions at $\sqrt{s} = 14$ TeV at LHC. We present the results of total cross section of diphotons, invariant mass distribution of the diphotons and p_T distribution of the diphotons and ZZ pairs from Higgs from string balls and black holes at LHC. We find that if string mass scale $M_s \sim$ TeV then the total cross section of diphotons from Higgs from string balls is larger than that from standard model Higgs. The result is more striking for the case of black holes where the total cross section of diphotons from Higgs from black holes is larger than that from standard model Higgs plus background processes. We find that the invariant mass distribution of the diphotons from Higgs from string balls and black holes is not very sensitive to the increase in diphoton invariant mass. We also find that $\frac{d\sigma}{dp_T}$ of high p_T diphotons and ZZ pairs produced from Higgs from string balls and black holes is larger than that from standard model Higgs, and also from diphotons and ZZ pairs produced directly from parton fusion processes at LHC. We observe that $\frac{d\sigma}{dp_T}$ of diphotons and ZZ pairs from Higgs from black holes increases with increase in p_T, whereas from Higgs from string balls it does not decrease sharply with increase in p_T, and from NLO pQCD Higgs it decreases rapidly. Hence the measurement of diphotons and ZZ pairs at LHC can be used to distinguish between Higgs production from: 1) black holes, 2) string balls and 3) parton fusion processes at CERN LHC.

PACS numbers: PACS: 04.70.Bw; 04.70.Dy; 12.38.Bx; 13.85.Ni; 14.65.Ha

---

[*] Electronic address: nayak@physics.arizona.edu

I. INTRODUCTION

One of the primary goal of the LHC experiment at CERN is to search for Higgs boson which is the last missing particle of the standard model of particle physics. Higgs is responsible for generating particle masses. It is now generally accepted that the scale of quantum gravity *could be* as low as one TeV [1–19]. In the presence of extra dimensions, the string mass scale M_s and the Planck mass M_P could be around $\sim$ TeV and we may expect to discover exotic physics at LHC such as mini-black holes and TeV scale string balls. Pragmatically we can only search for Higgs, extra dimensions, black holes and string balls at LHC in whatever mass range and energy range currently available at experiments. While detection of Higgs makes the standard model complete, the production of mini-black holes will establish the existence of extra dimensions and could possibly provide an experimental test of the quantum theory of gravity. Similarly, detection of string balls will provide experimental test of string theory for the first time. Hence if Higgs, black holes and string balls are discovered at LHC then we will be propelled into the twenty first century, as our understanding of quantum gravity and perhaps string theory is revolutionized. Once black holes and string balls are produced at LHC they will quickly evaporate to standard model particles including Higgs. Hence Higgs boson production from black holes and string balls at LHC can play an important role in distinguishing between Higgs from standard model electroweak physics and from quantum gravity and/or from string theory. For example, if we do not find Higgs from standard model processes at LHC but find from the decay of black holes and/or string balls then Higgs discovery at LHC may be related to gravity and/or string theory rather than to the standard model of electroweak theory. This may provide a basis to investigate Higgs mechanism in string theory and gravity [20–27]. Hence Higgs production from black holes and string balls at LHC will have important consequences for the physics of standard model, beyond standard model, quantum gravity and string theory. In this paper we make a detail analysis of the Higgs production from black holes and string balls at LHC and make a comparison with the Higgs production from standard model processes.

Recently, string theory has given convincing microscopic calculation for black hole evaporation [28, 29]. String theory predicts that a black hole has formed at several times the Planck scale and any thing smaller will dissolve into some thing known as string ball [30]. A string ball is a highly excited long string which emits massless (and massive) particles at

Hagedorn temperature with thermal spectrum [31, 32]. For general relativistic description of the back hole to be valid, the black hole mass M_{BH} has to be larger than the Planck mass M_P. In string theory the string ball mass M_{SB} is larger than the string mass scale M_s. Typically

$$M_s < M_P < \frac{M_s}{g_s^2}, \qquad M_s << M_{SB} << \frac{M_s}{g_s^2}, \qquad \frac{M_s}{g_s^2} << M_{BH} \tag{1}$$

where g_s is the string coupling which can be less than 1 for the string perturbation theory to be valid.

Since string ball is lighter than black hole, more string balls are expected to be produced at LHC than black holes. The Hagedorn temperature of a string ball is given by

$$T_{SB} = \frac{M_s}{\sqrt{8}\pi}. \tag{2}$$

The Hawking temperature of a black hole is [3]

$$T_{BH} = \frac{n+1}{4\pi R_{BH}} = \frac{n+1}{4\sqrt{\pi}} M_P [\frac{M_P}{M_{BH}} \frac{n+2}{8\Gamma(\frac{n+3}{2})}]^{\frac{1}{1+n}}, \tag{3}$$

where R_{BH} is the Schwarzschild radius of the black hole, M_{BH} is the black hole mass and n is the number of extra dimensions. Since these temperatures are very high at LHC ($\sim$ hundreds of GeV) we expect more massive particles ($M \sim 3T$) to be produced at CERN LHC from string balls/black holes.

The main channel for direct Higgs production at LHC at $\sqrt{s} = 14$ TeV is via parton (gluon) fusion processes. The differential cross section for Higgs production in pp collisions at LHC is given by [33–35]

$$d\sigma = \sum_{a,b=q,\bar{q},g} \int dx_1 \int dx_2 \ f_{a/P}(x_1,\mu^2) \ f_{b/P}(x_2,\mu^2) d\hat{\sigma}_{ab} \tag{4}$$

where $d\hat{\sigma}_{ab}$ is differential cross section for Higgs production in parton fusion processes. There are contributions from WW/ZZ fusion processes to inclusive Higgs production at LHC but their contributions will be small, see below, where we also make a comparison with the other backgrounds to standard model Higgs production at LHC.

As discussed in [36–38] there is another mode of Higgs production which is via Hawking's radiation of black holes at LHC. The decay of Higgs which are produced from black holes is studied in [39]. In this paper we make a detail analysis of Higgs production and decay from string balls at LHC. We make a comparison of this with the Higgs production and decay from from black holes and with the standard model Higgs.

It is useful to mention that the Higgs mass is not predicted by the standard model. Although indirect electroweak precession data rules out a heavy Higgs of mass M_H=200 GeV, the exact mass of Higgs remains unknown unless we discover Higgs. Higgs mass up to 550 GeV or more will be searched at ATLAS [40] and CMS detectors [41, 42] at LHC. Furthermore a Higgs of mass 200 GeV is allowed in the string ball and/or black hole decay. Hence it is desirable to make theoretical predictions at LHC with light Higgs as well as heavy Higgs. For this reason we have performed our calculation with light Higgs decaying to diphoton and heavy Higgs decaying to ZZ pair. For light Higgs decay we mainly focus on diphoton decay channel with Higgs mass $M_H = 120$ GeV. For the heavy Higgs decay we focus on ZZ golden decay channel with Higgs mass $M_H = 200$ GeV.

The paper is organized as follows. In section II we briefly describe Higgs production and decay from string balls and from black holes at LHC. In section III we present the results and discussions and conclude in section IV.

II. HIGGS PRODUCTION AND DECAY FROM STRING BALLS VS BLACK HOLES AT LHC

The differential cross section for Higgs with mass M_H, momentum $\vec{p}$ and energy $E = \sqrt{\vec{p}^2 + M_H^2}$ from a black hole of temperature T_{BH} is given by [39]

$$\frac{Ed\sigma_{\rm Higgs}}{d^3p} = \frac{1}{(2\pi)^3 s}\sum_{ab} \int_{\frac{M_s^2}{g_s^4}}^{s} dM^2 \int \frac{dx_a}{x_a}\, f_{a/p}(x_a,\mu^2)\, f_{b/p}(\frac{M^2}{sx_a},\mu^2)\, \hat{\sigma}^{ab}(M)\, \frac{c_n\sigma_n\gamma\tau_{BH}p^\mu u_\mu}{(e^{\frac{p^\mu u_\mu}{T_{BH}}}-1)}, \tag{5}$$

where M_s is the string mass scale and g_s is the string coupling which is less than 1 for the string perturbation theory to be valid, see eq. (1). The flow velocity is u^μ and γ is the Lorentz boost factor with

$$\gamma\vec{v}_{BH} = (0, 0, \frac{(x_1 - x_2)\sqrt{s}}{2M_{BH}}). \tag{6}$$

We take the grey body factor σ_n in the geometrical approximation [43]

$$\sigma_n = \pi\left(\frac{n+3}{2}\right)^{2/(n+1)} \frac{n+3}{n+1} R_{\rm BH}^2. \tag{7}$$

The partonic level cross section of the black hole can be approximated with the pure geometrical form $\hat{\sigma}^{ab}(M_{BH}) \sim \pi R_{BH}^2$. The multiplicity factor $c_n = 1$ for Higgs because there is no color or spin degrees of freedom [14]. The decay time of the black hole is given by [39]

$$\tau_{BH} = \frac{1}{M_P}(\frac{M_{BH}}{M_P})^{\frac{n+3}{n+1}}. \tag{8}$$

Similarly, the differential cross section for Higgs with mass M_H, momentum $\vec{p}$ and energy $E = \sqrt{\vec{p}^2 + M_H^2}$ from a string ball of temperature T_{SB} is given by

$$\frac{Ed\sigma_{\rm Higgs}}{d^3p} = \frac{1}{(2\pi)^3 s}\sum_{ab} \int_{M_s^2}^{\frac{M_s^2}{g_s^4}} dM^2 \int \frac{dx_a}{x_a}\ f_{a/p}(x_a,\mu^2)\ f_{b/p}(\frac{M^2}{sx_a},\mu^2)\ \hat{\sigma}^{ab}(M)\ \frac{A_n c_n \gamma \tau_{SB} p^\mu u_\mu}{(e^{\frac{p^\mu u_\mu}{T_{SB}}}-1)}, \tag{9}$$

where A_n is the $d(= n+3)$ dimensional area factor [44, 45]. We will use the number of extra dimensions $n = 6$ in our calculation. The partonic level string ball production cross section is given by [30]

$$\begin{aligned} \hat{\sigma}(M_{SB}) &= \frac{1}{M_s^2}, & \frac{M_s}{g_s} < M_{SB} < \frac{M_s}{g_s^2} \\ \hat{\sigma}(M_{SB}) &= \frac{g_s^2 M_{SB}^2}{M_s^4}, & M_s < M_{SB} < \frac{M_s}{g_s}. \end{aligned} \tag{10}$$

We have used CTEQ6M PDF [46] in our calculation.

We consider diphoton and ZZ decay channel of Higgs at LHC when the Higgs is produced from string balls and black holes and make a comparison with the diphoton and ZZ produced from standard model Higgs and with the direct diphoton and ZZ production from standard model processes. The branching ratio of Higgs decay is function of Higgs mass [47]. As the temperature of the string ball (black hole) is very large at LHC there is not much difference in the Higgs production cross section from string balls (black holes) if the Higgs mass M_H is increased from 100 to 300 GeV. As mentioned above the string coupling g_s should be less than 1 for the string perturbation theory to be valid, see eq. (1). Hence we will use [30, 32]

$$g_s^2 = \frac{1}{3} \tag{11}$$

in our calculation.

III. RESULTS AND DISCUSSIONS

In this section we present the results of Higgs production and decay in pp collisions at $\sqrt{s}$ = 14 TeV at LHC. For Higgs decay we study invariant mass spectrum of diphoton and p_T

distribution of diphoton and ZZ pair. We also present the results of diphoton cross section from Higgs deacy at LHC.

The details about p_T measurement, resolution and implication for the Higgs signal is avalable in ATLAS technical design report on $\frac{d\sigma}{dM_{\gamma\gamma}}$, $\frac{d\sigma}{dp_T^{\gamma\gamma}}$ and $\sigma_{\gamma\gamma}$ measurements [48–50]. In the mass range $110 < m_H < 140$ GeV the Higgs boson is expected to decay into two photons with a branching fraction large enough to render the search feasible at LHC [51]. For this reason we present our results of $\frac{d\sigma}{dM_{\gamma\gamma}}$ in the diphoton invariant mass range $110 < M_{\gamma\gamma} < 140$ GeV. Applied transverse momentum cuts are from ATLAS [48, 50]. For CMS transverse momentum cuts, see [52]. The $\frac{d\sigma}{dp_T}$ of diphoton from Higgs at ATLAS is expected to be measured up to $p_T \sim 200$ GeV, see [48, 49]. If black holes and Higgs are discovered at LHC then there may be upgrade at ATLAS to measure $\frac{d\sigma}{dp_T}$ of Higgs up to $p_T \sim$ TeV. This may be the case in the reverse scenario as well. For example, if we do not find Higgs in the present experimental set up at ATLAS then there may be upgrade at ATLAS to extend p_T measurement up to TeV. For this reason we have considered a wide range of p_T in this paper which covers the ATLAS range as given in [48, 49].

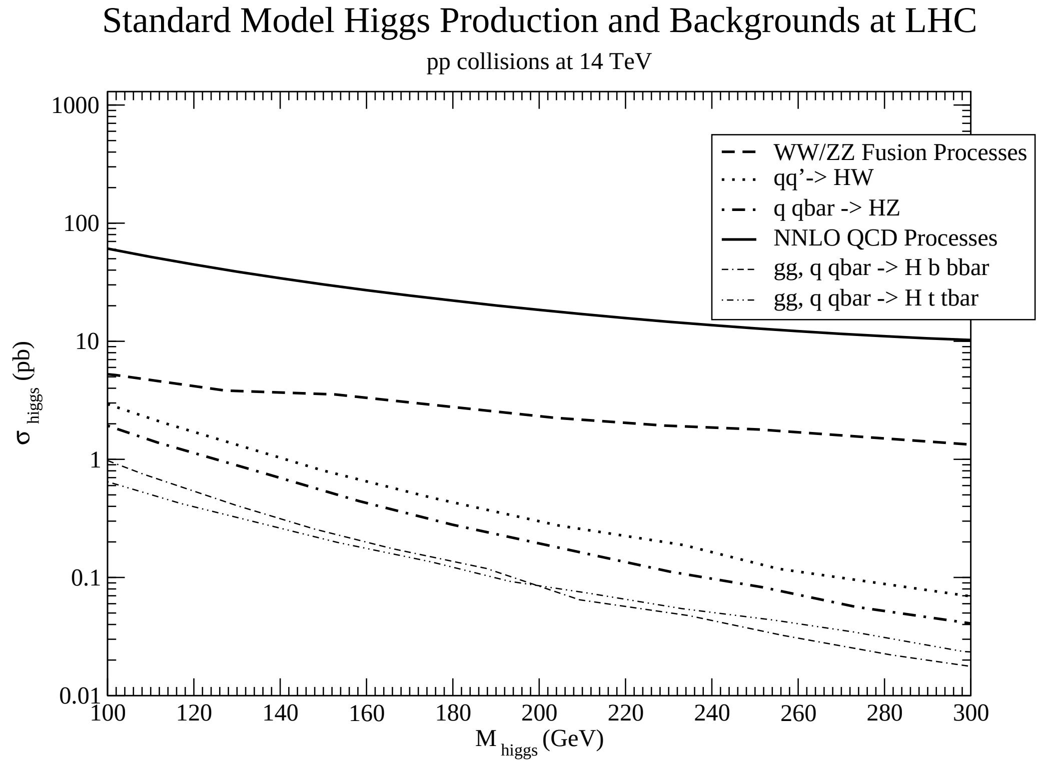

FIG. 1: Total cross section for Higgs production from parton fusion processes using pQCD at NNLO and the Higgs production from other standard model processes at LHC.

A. Higgs Production at LHC

In Fig.1 we present total Higgs production cross section at LHC from parton fusion processes at NNLO using pQCD. We also present the results from WW/ZZ fusion processes and other backgrounds to standard model Higgs production at LHC. As can be seen from the figure the main contribution is from parton fusion processes at LHC, the gluon fusion process being the dominant one. The solid line is for Higgs cross section from QCD reactions using parton fusion processes at NNLO by using pQCD [34]. There are contributions from the so-called weak boson fusion reactions involving coupling of W and Z bosons to Higgs. In the later case a typical parton reaction is $qq \rightarrow Hqq$ where two virtual Z-bosons are exchanged between the quarks and Higgs. This is a typical t-channel process. The virtual W^+ and W^- bosons can also be exchanged. This so called WW/ZZ reaction is not dominate at LHC. The dashed line is for the process $qq \rightarrow Hqq$. The dotted line is for the process $qq' \rightarrow HW$ and the dot-dashed line is for the process $q\bar{q} \rightarrow HZ$ respectively. The dot-dashed-dashed line is for the process $gg,\ q\bar{q} \rightarrow Hb\bar{b}$ and dot-dot-dashed line is for the process $gg,\ q\bar{q} \rightarrow Ht\bar{t}$ respectively. All the backgrounds to standard model Higgs production at LHC are taken from [47]. It can be seen that the parton fusion processes (the solid line) gives the dominant contribution to the Higgs production at LHC. Hence we will only consider parton fusion results when we make comparisons of the total cross section σ with the Higgs production from string balls and black holes at LHC.

In Fig.2 we present the results of $\frac{d\sigma}{dp_T}$ of Higgs cross section at LHC from parton fusion processes at NLO using pQCD and compare it with WW/ZZ fusion reactions. The solid line is from parton fusion processes and the dashed line is from WW/ZZ fusion processes. The p_T distributions of Higgs at LHC from WW/ZZ fusion reactions at NLO are taken from [53]. It can be seen that WW/ZZ reaction is not the dominate contribution to *inclusive* Higgs production at large p_T at LHC. Hence we will only consider parton fusion results when we make comparisons of $\frac{d\sigma}{dp_T}$ with the Higgs production from string balls and black holes at LHC. If one identifies the two final state jets and applies p_T cuts on them then it is possible to enhance the weak boson signal and decrease the QCD signal. However, this now involves the study of exclusive processes which is not the subject of this paper.

In Fig.3 we present total Higgs production cross section from string balls and compare them with the pQCD predictions at NNLO. The former is given by the solid line with string

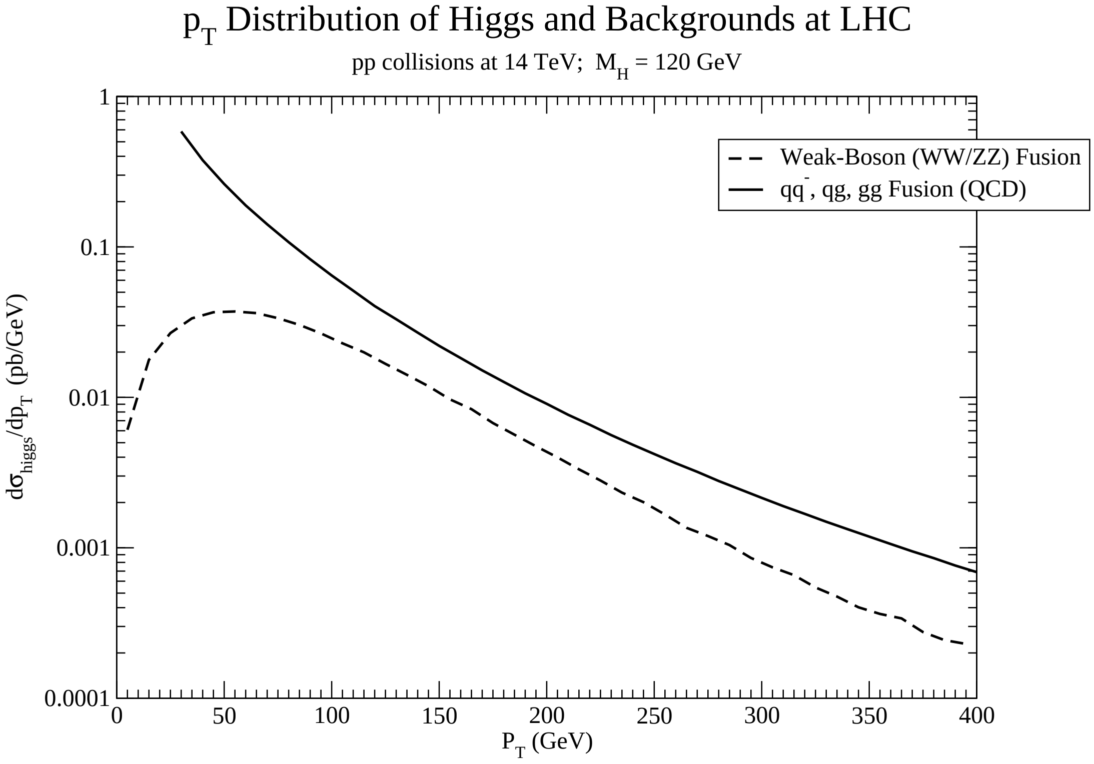

FIG. 2: p_T distribution of the Higgs production from parton fusion processes using pQCD at NLO and from WW/ZZ fusion processes at NLO at LHC.

mass scale $M_s = 1$ TeV. We plot for comparison the NNLO Higgs cross section [34]. The dotted line is for NNLO pQCD Higgs cross section at LHC. It is clear that if string mass scale is $\sim$ TeV then the total Higgs cross section from string balls is larger than pQCD cross section.

In Fig.4 we present $\frac{d\sigma}{dp_T}$ of Higgs production from string balls at LHC and compare them with the pQCD predictions at NLO. The Higgs mass is chosen to be 120 GeV from the string balls decay. We plot for comparison the NLO results for $\frac{d\sigma}{dp_T}$ of Higgs using pQCD [35]. The thin-dotted line is the NLO pQCD result with Higgs mass 120 GeV. The dashed line is the NLO pQCD result with Higgs mass 160 GeV. The dot-dot-dashed line is the NLO pQCD result with Higgs mass 200 GeV. The solid line is for $\frac{d\sigma}{dp_T}$ of Higgs from string balls with string mass scale M_s equal to 1 TeV and Higgs mass equal to 120 GeV. It is clear that if the string mass scale is $\sim$ TeV then $\frac{d\sigma}{dp_T}$ of the Higgs via string ball decay is larger than the standard model pQCD predictions for larger values of p_T ($p_T > 100$ GeV) of Higgs. We observe that for larger values of p_T, $\frac{d\sigma}{dp_T}$ of Higgs from string balls does not sharply decrease

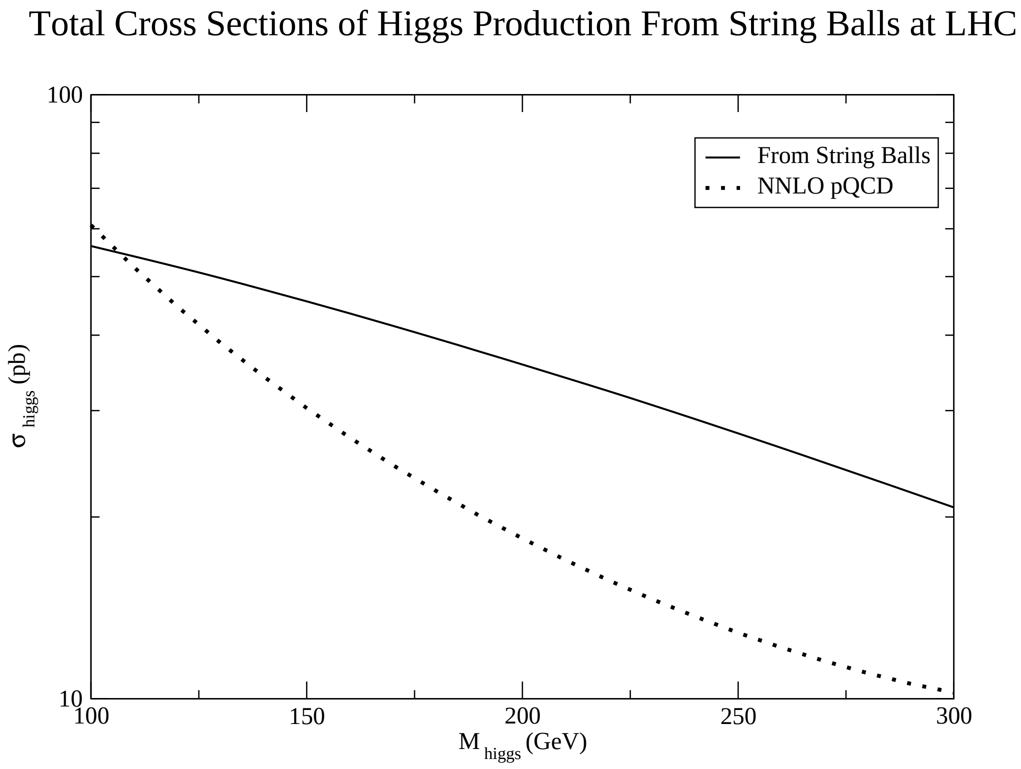

FIG. 3: Total cross section for Higgs production at LHC from string balls and from direct pQCD processes at NNLO.

with increasing p_T, whereas in case of NLO pQCD processes it decreases rapidly.

In Fig.5 we present total Higgs production cross section from black holes at LHC and compare with the Higgs cross sections from NNLO pQCD processes. The dashed line is for Higgs production from black holes with string mass scale $M_s = 1$ TeV. We plot for comparison the NNLO Higgs cross section [34]. The solid line is for NNLO cross section. It is clear that if the string mass scale is $\sim$ TeV then the total Higgs cross section from black holes is much larger than NNLO pQCD cross section and is not sensitive to the increase in Higgs mass.

In Fig.6 we present $\frac{d\sigma}{dp_T}$ of Higgs production from black holes and compare them with the pQCD predictions of Higgs at NLO. Since the Higgs cross section from black holes decay is not sensitive to the Higgs mass (see Fig. 5) we have chosen the Higgs mass equal to 120 GeV. We plot for comparison the NLO results for $\frac{d\sigma}{dp_T}$ of Higgs using pQCD [35]. The solid line is Higgs production from black holes with string mass scale $M_s = 1$ TeV. The dotted line is for Higgs production from NLO pQCD processes with M_H =120 GeV. The

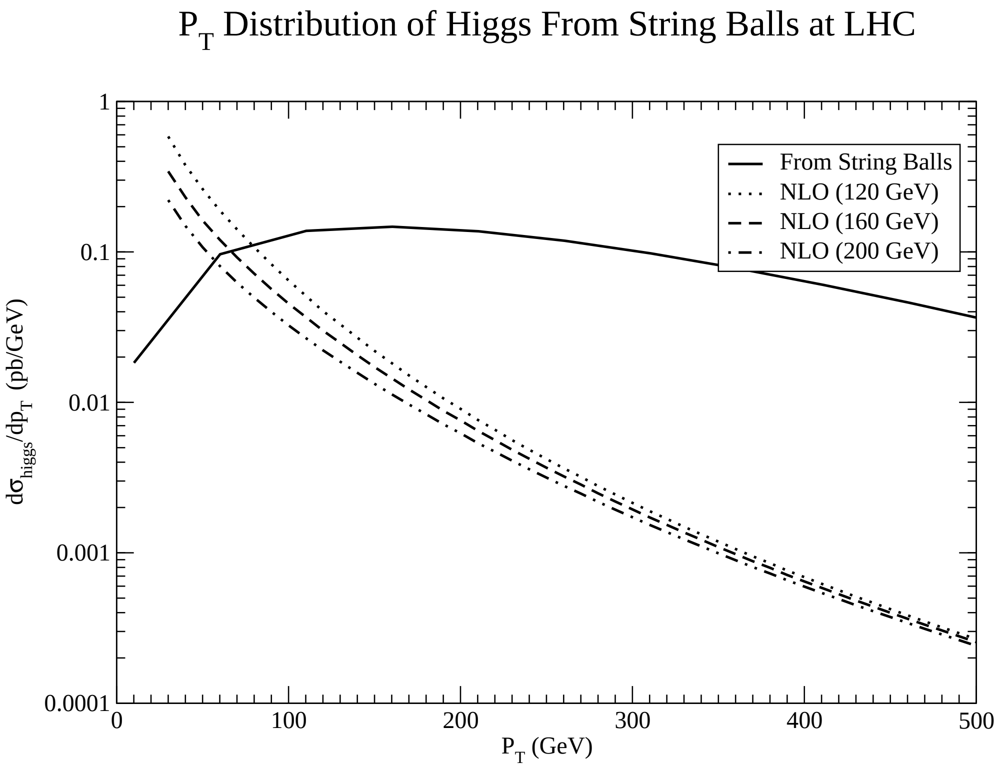

FIG. 4: p_T distribution of Higgs production at LHC from string balls and from direct pQCD processes at NLO.

thin-solid line is for Higgs production from NLO pQCD processes with M_H =160 GeV and the dot-dot-dashed line is for M_H = 200 GeV respectively. It is clear that if the string mass scale is $\sim$ TeV then the $\frac{d\sigma}{dp_T}$ of the Higgs from black holes at LHC is larger than the standard model pQCD predictions for larger values of p_T ($p_T \geq 70$ GeV). For larger values of p_T, the $\frac{d\sigma}{dp_T}$ of Higgs from black holes increases with increasing p_T for p_T up to $\sim$ 250 GeV and then remains almost constant. On the other hand the $\frac{d\sigma}{dp_T}$ of Higgs from NLO pQCD processes decreases rapidly. In case of string balls, the $\frac{d\sigma}{dp_T}$ does not decrease sharply with increasing p_T (see Fig. 4).

B. Higgs Decay at LHC

The branching ratio of Higgs decay is a function of Higgs mass [47]. We present the results of invariant mass spectrum of diphoton and p_T distribution of $\gamma\gamma$ and ZZ pair from Higgs from string balls and black holes at LHC. We also compute diphoton cross section from Higgs decay from black holes and string balls at LHC.

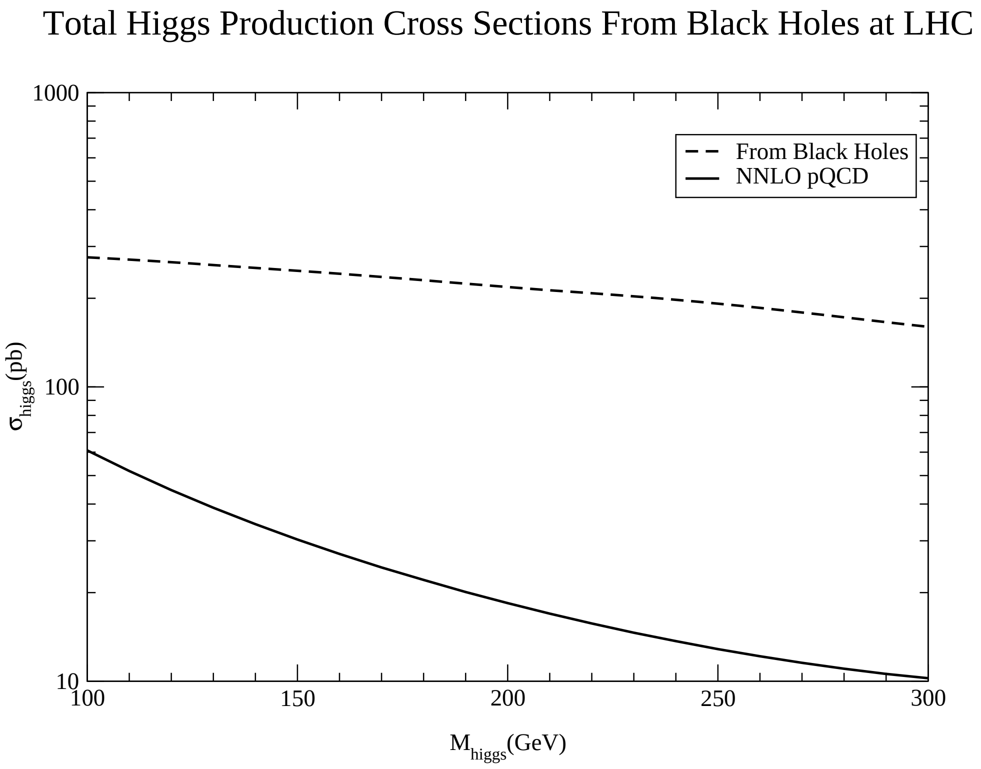

FIG. 5: Total Higgs cross sections at LHC from black holes and from direct pQCD processes at NNLO.

1. p_T Distribution of Diphoton and ZZ Pair From Higgs Decay at LHC

In this section we present the results of $\frac{d\sigma}{dp_T}$ of diphoton and ZZ pair production from Higgs from string balls (black holes) and from Higgs in parton fusion processes at NLO. We also compare these with the $\frac{d\sigma}{dp_T}$ of diphoton and ZZ pairs directly produced from parton fusion processes at LHC [54, 55]. For the diphoton channel we consider light Higgs with mass $M_H = 120$ GeV and for ZZ decay channel we consider heavy Higgs with mass $M_H = 200$ GeV.

In Fig.7 we present the results of $\frac{d\sigma}{dp_T}$ of diphoton production from Higgs from black holes and make a comparison with the diphoton produced from Higgs from parton fusion processes at LHC and with the $\frac{d\sigma}{dp_T}$ of diphoton produced directly from parton fusion processes at LHC [54]. We have used the Higgs mass $M_H = 120$ GeV in our calculation for diphoton case. The dotted line is for diphoton from Higgs from black holes with string mass scale $M_s = 1$ TeV. The dot-dashed line is for diphoton from Higgs where the Higgs is produced from parton fusion processes at LHC. The dashed line is for $\frac{d\sigma}{dp_T}$ of diphoton produced directly

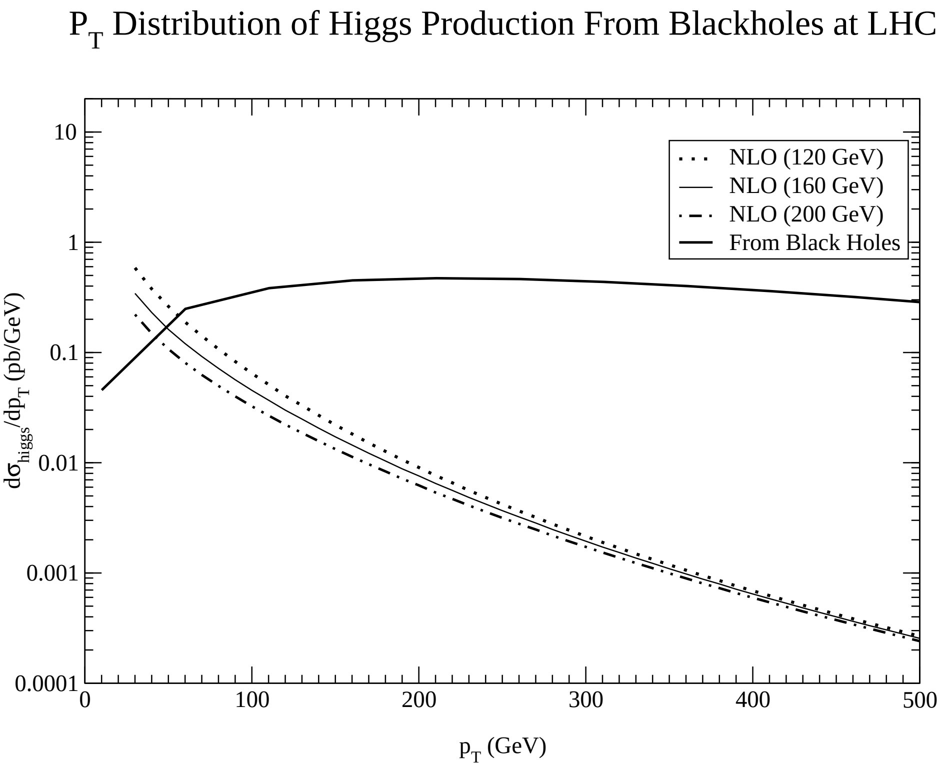

FIG. 6: p_T distribution of Higgs production at LHC from black holes and from direct pQCD processes at NLO.

from parton fusion processes at LHC [54]. It can be seen that if string mass scale is $\sim$ TeV then the $\frac{d\sigma}{dp_T}$ of diphoton production from Higgs from black holes is larger than $\frac{d\sigma}{dp_T}$ of diphotons produced from the standard model Higgs for $p_T \geq 70$ GeV. Although the diphoton p_T distribution from direct parton fusion processes in [54] is not available at very high p_T ($\sim$ 200 GeV - 500 GeV) at LHC, the trend in decrease of $\frac{d\sigma}{dp_T}$ of diphoton from direct QCD processes suggests that it may be less than diphotons from Higgs from black holes for very high p_T of diphotons ($p_T \sim 300$ GeV) at LHC.

Hence we find that $\frac{d\sigma}{dp_T}$ of high p_T ($\sim$ 300-500 GeV) diphotons from Higgs from black holes at LHC can be larger than $\frac{d\sigma}{dp_T}$ of diphotons from standard model Higgs and also can be larger than $\frac{d\sigma}{dp_T}$ of diphotons from direct pQCD processes if the the string mass scale $M_s \sim 1$ TeV. We find that for larger values of p_T, $\frac{d\sigma}{dp_T}$ of diphotons from Higgs from black holes increases with increasing p_T for p_T up to $\sim$ 250 GeV and then remains constant. On the other hand $\frac{d\sigma}{dp_T}$ of diphotons from Higgs from NLO pQCD processes decreases rapidly.

In Fig.8 we present the results of $\frac{d\sigma}{dp_T}$ of diphoton production from Higgs from string

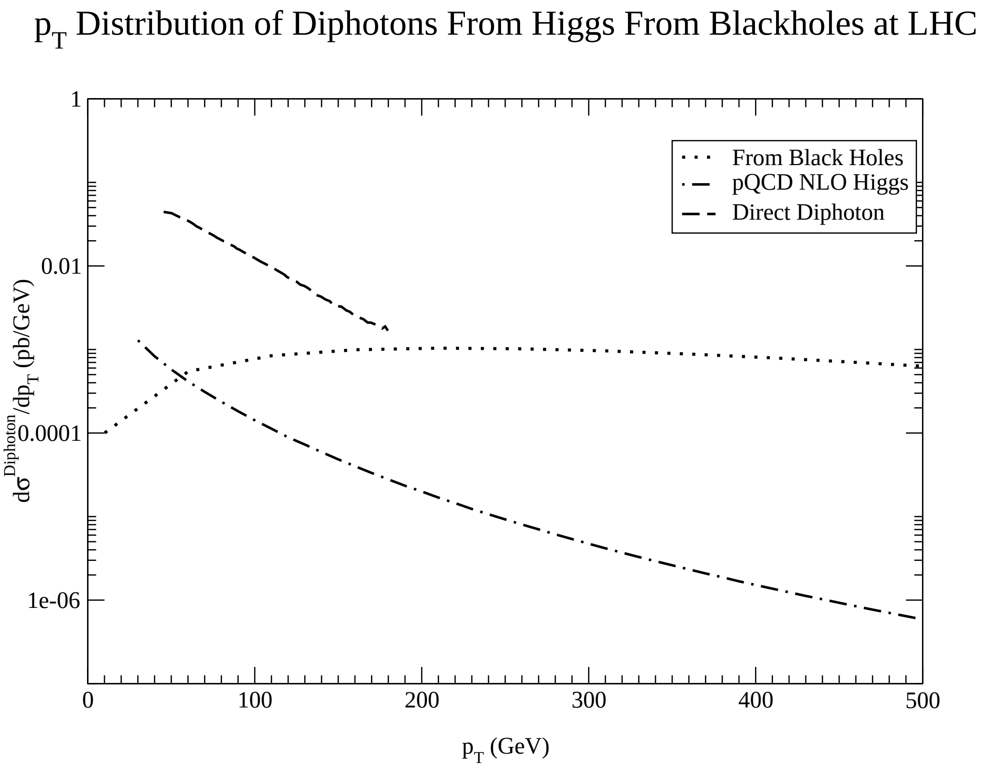

FIG. 7: p_T distribution of diphoton production from Higgs from black holes at LHC and from Higgs from parton fusion processes using pQCD at LHC.

balls and make a comparison with the diphoton produced from Higgs from parton fusion processes at LHC and with $\frac{d\sigma}{dp_T}$ of diphoton produced directly from parton fusion processes at LHC [54]. The dashed line is for diphoton from Higgs from string balls with string mass scale M_s = 1 TeV. The solid line is for diphoton from Higgs where the Higgs is produced from parton fusion processes at LHC. The dot-dashed line is for $\frac{d\sigma}{dp_T}$ of diphotons produced directly from parton fusion processes at LHC [54]. It can be seen that for $p_T \geq 100$ GeV, $\frac{d\sigma}{dp_T}$ of diphoton production from Higgs from string balls is larger than $\frac{d\sigma}{dp_T}$ of diphotons produced from standard model Higgs if the string mass scale $M_s \sim 1$ TeV. Although $\frac{d\sigma}{dp_T}$ of diphotons from direct parton fusion processes in [54] is not available at very high p_T ($\sim$ 200 GeV - 500 GeV) at LHC, the trend in decrease of $\frac{d\sigma}{dp_T}$ of diphoton from direct QCD processes suggests that it may be less than $\frac{d\sigma}{dp_T}$ of diphotons from Higgs from string balls for p_T of diphoton $\geq$ 300 GeV at LHC if $M_s \sim$1 TeV.

Hence we find that $\frac{d\sigma}{dp_T}$ of high p_T ($\sim$ 300-500 GeV) diphoton from Higgs from string balls at LHC can be larger than $\frac{d\sigma}{dp_T}$ of diphotons from standard model Higgs and also can

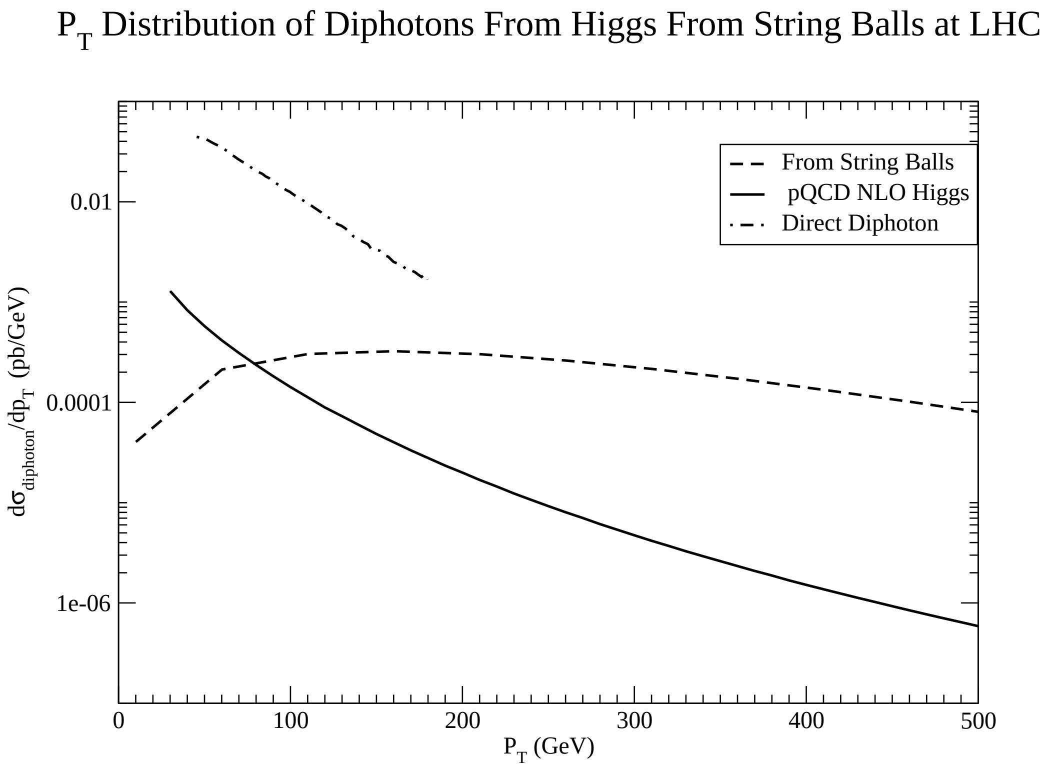

FIG. 8: p_T distribution of diphoton production from Higgs from string balls at LHC and from Higgs from parton fusion processes using pQCD at LHC

.

be larger than $\frac{d\sigma}{dp_T}$ of diphotons from direct parton fusion processes if the the string mass scale $M_s \sim 1$ TeV. We find that for larger values of p_T, $\frac{d\sigma}{dp_T}$ of diphotons from Higgs from string balls does not decrease sharply with increase in p_T, whereas in case of NLO pQCD processes it decreases rapidly. On the other hand $\frac{d\sigma}{dp_T}$ of diphotons from Higgs from black holes increases with increasing p_T (see Fig. 7).

In Fig.9 we present the results of $\frac{d\sigma}{dp_T}$ of ZZ pairs produced from Higgs from black holes and make a comparison with the ZZ produced from Higgs from parton fusion processes at LHC and with $\frac{d\sigma}{dp_T}$ of ZZ pairs produced directly from parton fusion processes at LHC [55]. We have used the Higgs mass $M_H = 200$ GeV in our calculation for ZZ case. The dotted line is for ZZ from Higgs from black holes with string mass scale $M_s = 1$ TeV. The dot-dashed line is for ZZ from Higgs where the Higgs is produced from parton fusion processes at LHC. It can be seen that for $p_T \geq 70$ GeV the $\frac{d\sigma}{dp_T}$ of ZZ pairs produced from Higgs from black holes is larger than $\frac{d\sigma}{dp_T}$ of ZZ pairs produced from the standard model Higgs and also is

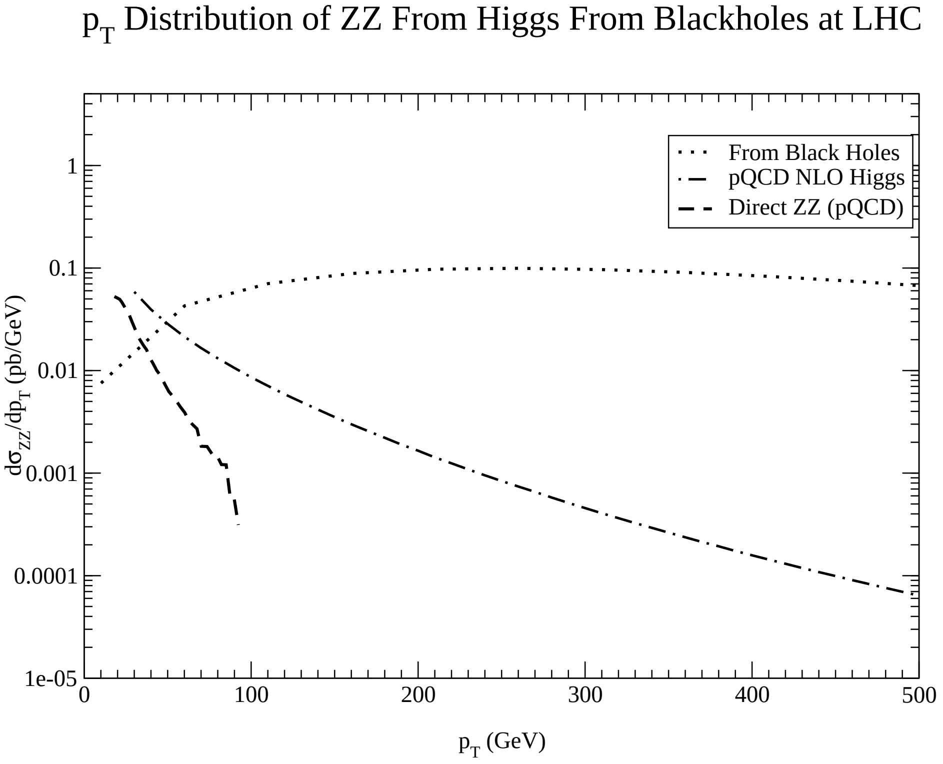

FIG. 9: p_T distribution of ZZ pair production from Higgs from black holes at LHC and from Higgs from parton fusion processes using pQCD at LHC.

larger than $\frac{d\sigma}{dp_T}$ of ZZ pairs from direct parton fusion processes if the string mass scale $M_s \sim$ 1 TeV.

Hence we find that $\frac{d\sigma}{dp_T}$ of ZZ pairs produced from Higgs from black holes at LHC can be larger than $\frac{d\sigma}{dp_T}$ of ZZ pairs produced from standard model Higgs and also can be larger than $\frac{d\sigma}{dp_T}$ of ZZ pairs produced from direct parton fusion processes if the the string mass scale $M_s \sim 1$ TeV. We find that for larger values of p_T, $\frac{d\sigma}{dp_T}$ of ZZ pairs produced from Higgs from black holes increases with increasing p_T, whereas in case of NLO pQCD processes it decreases rapidly.

In Fig.10 we present the results of $\frac{d\sigma}{dp_T}$ of ZZ pairs produced from Higgs from string balls and make a comparison with the ZZ produced from Higgs from parton fusion processes at LHC and with the $\frac{d\sigma}{dp_T}$ of ZZ pairs produced directly from parton fusion processes at LHC [55]. We have used the Higgs mass $M_H = 200$ GeV in our calculation for the ZZ case. The dashed line is for ZZ from Higgs from string balls with string mass scale $M_s = 1$ TeV. The solid line is for ZZ from Higgs where the Higgs is produced from parton fusion processes

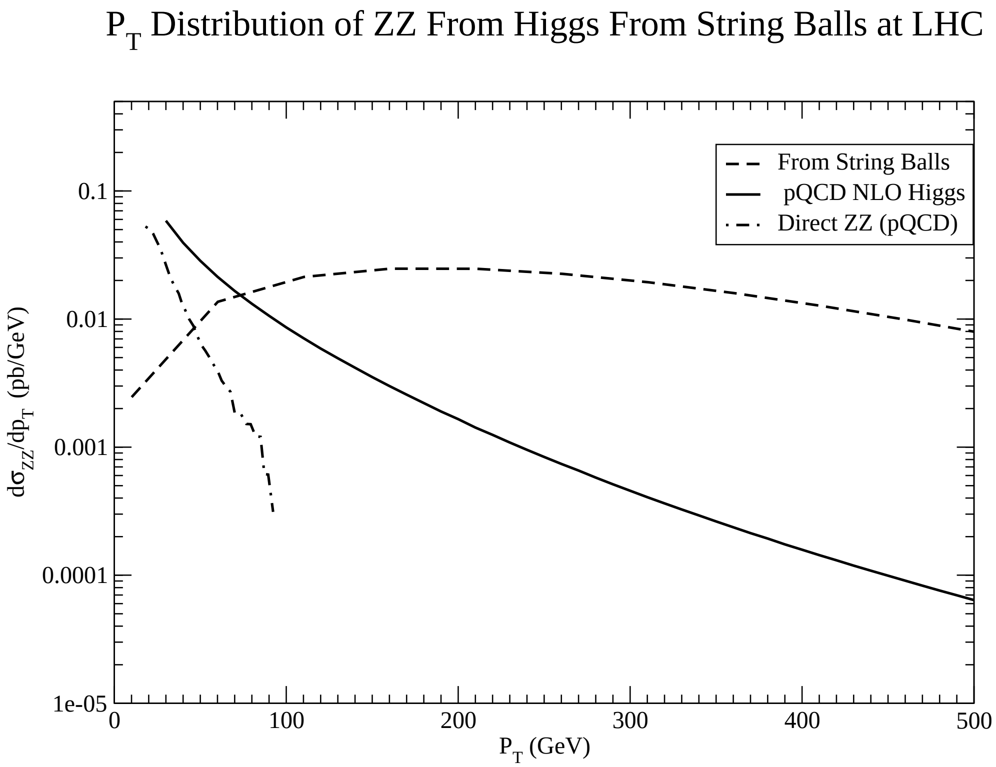

FIG. 10: p_T distribution of ZZ pair production from Higgs from string balls at LHC and from Higgs from parton fusion processes using pQCD at LHC.

at LHC. The dot-dashed line is the $\frac{d\sigma}{dp_T}$ of ZZ pairs produced directly from parton fusion processes at LHC [55]. It can be seen that for $p_T \geq 100$ GeV, $\frac{d\sigma}{dp_T}$ of ZZ pairs produced from Higgs from string balls is larger than $\frac{d\sigma}{dp_T}$ of ZZ pairs produced from standard model Higgs and also is larger than $\frac{d\sigma}{dp_T}$ of ZZ pairs produced from direct parton fusion processes if the string mass scale $M_s \sim 1$ TeV.

Hence we find that for $p_T \geq 100$ GeV, $\frac{d\sigma}{dp_T}$ of ZZ pairs produced from Higgs from string balls at LHC can be larger than $\frac{d\sigma}{dp_T}$ of ZZ pairs produced from standard model Higgs and also can be larger than $\frac{d\sigma}{dp_T}$ of ZZ pairs produced from direct parton fusion processes if the the string mass scale $M_s \sim 1$ TeV. We find that for larger values of p_T, $\frac{d\sigma}{dp_T}$ of ZZ pairs from Higgs from string balls does not decrease sharply with increase in p_T, whereas in case of NLO pQCD processes it decreases rapidly. On the other hand $\frac{d\sigma}{dp_T}$ of ZZ from Higgs from black holes increases with increasing p_T (see Fig. 9).

These results suggest that if string mass scale $M_s \sim$ TeV then $\frac{d\sigma}{dp_T}$ of high p_T diphotons and ZZ pairs can be used to distinguish between Higgs production from: 1) black holes, 2) string balls and 3) parton fusion processes at CERN LHC.

2. Invariant Mass Spectrum of Diphoton From Higgs Decay at LHC

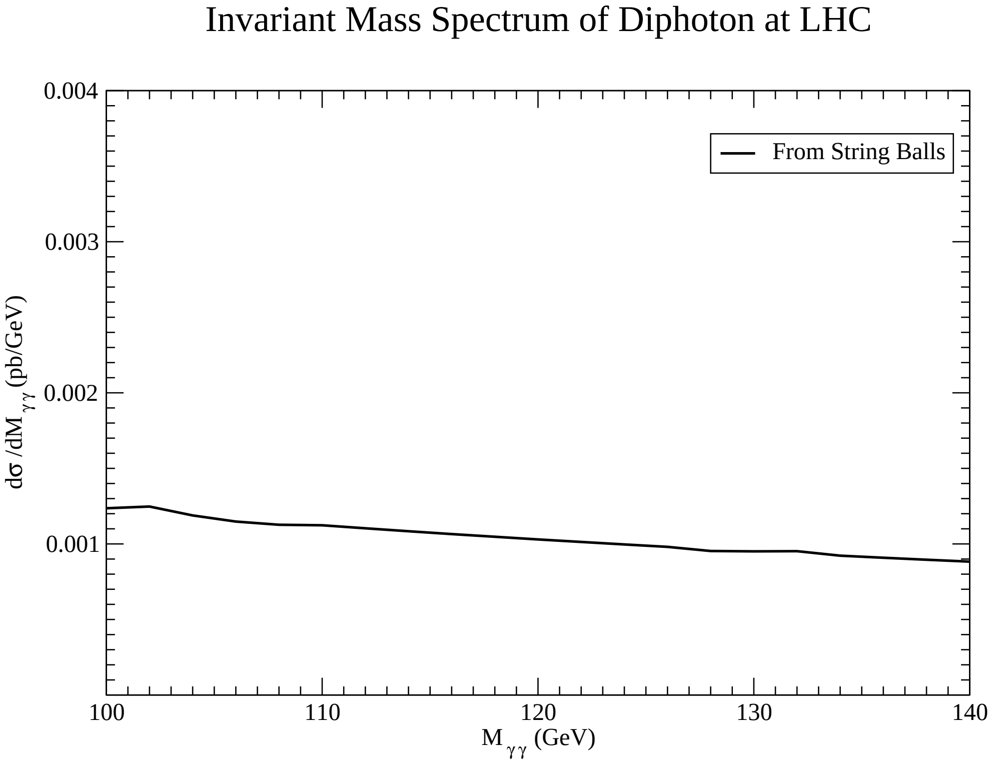

FIG. 11: Invariant mass spectrum of diphoton from Higgs from string balls at LHC.

In the mass range $110 < m_H < 140$ GeV the Higgs boson is expected to decay into two photons with a branching fraction large enough to render the search feasible at LHC [51]. For this reason we present our result of $\frac{d\sigma}{dM_{\gamma\gamma}}$ vs $M_{\gamma\gamma}$ in the diphoton invariant mass range $110 < M_{\gamma\gamma} < 140$ GeV. Note that we have used the branching ratio of Higgs decay which is a function of Higgs mass [47]. The applied transverse momentum cuts are from ATLAS [48, 50]. For transverse momentum cuts at CMS, see [52].

In Fig.11 we present $\frac{d\sigma}{dM_{\gamma\gamma}}$ of diphoton from Higgs from string balls at LHC as a function of diphoton invariant mass with string mass scale $M_s = 1$ TeV. Similarly, in Fig.12 we present $\frac{d\sigma}{dM_{\gamma\gamma}}$ of diphoton from Higgs from black holes at LHC as a function of diphoton invariant mass with string mass scale M_s=1 TeV. For the corresponding results from background processes and from standard model Higgs, see [48, 50]. Our results suggest that $\frac{d\sigma}{dM_{\gamma\gamma}}$ of diphoton from Higgs from string balls and black holes at LHC does not decrease rapidly as the diphoton invariant mass $M_{\gamma\gamma}$ increases.

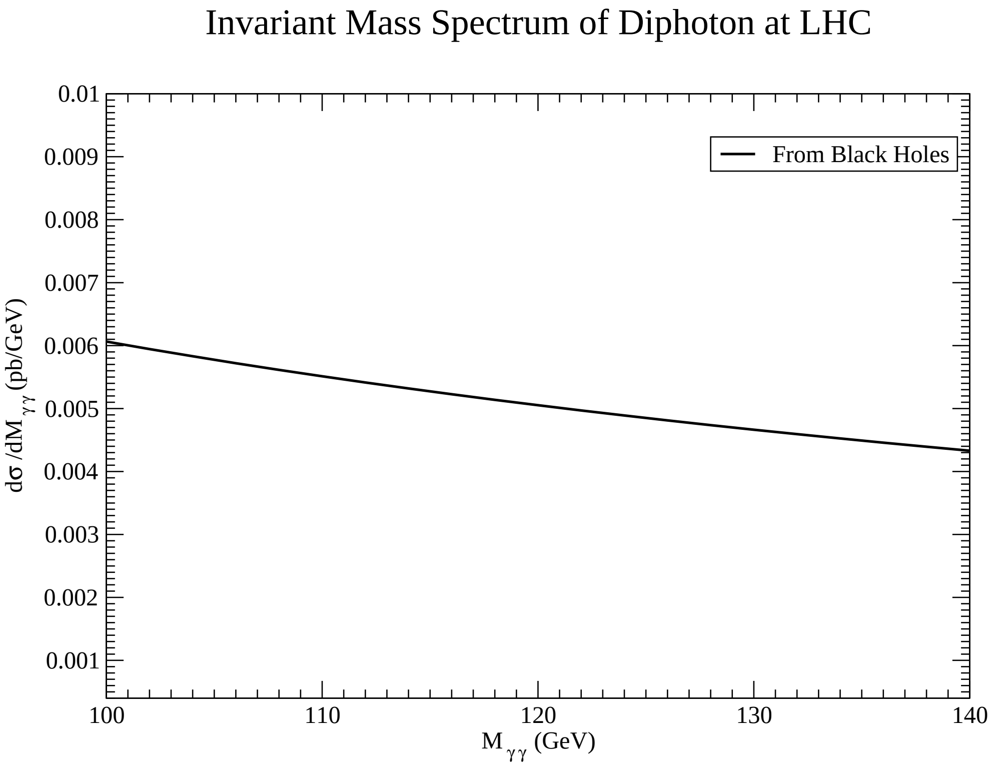

FIG. 12: Invariant mass spectrum of diphoton from Higgs from black holes at LHC.

3. *Diphoton Cross Section From Higgs Decay at LHC*

In table-I we present the results for diphoton cross sections at LHC from different signal (M_H=120 GeV) and background processes. For applied transverse momentum cuts and diphoton mass window at ATLAS, see [50].

It can be seen from table-I that the diphoton cross section from Higgs from string balls at LHC is larger than that from standard model Higgs when string mass scale M_s=1 TeV. It is also comparable to the diphoton cross section from background processes. The result is more striking from mini-black holes. For example, if string mass scale M_s=1 TeV then the diphoton cross section from Higgs from black holes is larger than that from standard model Higgs plus background processes.

Hence our results suggest that if string mass scale M_s is $\sim$ TeV then black holes and string balls will have significant effects on Higgs search at LHC.

$\gamma\gamma$ at LHC from:	Cross Section (fb)	$M_s = 1$ TeV
Background processes	562 [50]	
Standard model Higgs	25.3 [50]	
Higgs from string balls	110	
Higgs from black holes	616	

TABLE I: Diphoton cross section from different signal (Higgs) and background processes at LHC. For transverse momentum cuts and diphoton invariant mass window, see [50].

C. Current Experimental and Theoretical Constraints on M_s and M_P

High energy colliders have set lower limits on the Planck mass M_P at various experiments. The current limits from LEP2, CDF (run II) and D0 (run II) are as follows. The LEP2 analysis has set a lower limit on the Planck mass $M_P^{\rm min}$=1.69 TeV by using graviton production [56]. Search for large extra dimensions in the production of jets and missing transverse energy at CDF gives $M_P^{\rm min}$=0.83 TeV for n=6 to $M_P^{\rm min}$=1.18 TeV for n=2 [57], where n is the number of extra dimensions. The search for large extra dimensions in final states containing one photon or jet and large missing transverse energy at CDF gives $M_P^{\rm min}$=0.94 TeV for n=6 to $M_P^{\rm min}$=1.4 TeV for n=2 [58]. Dielectron and diphoton measurements at D0 gives $M_P^{\rm min}$=1.3 TeV for n=7 to $M_P^{\rm min}$=2.1 TeV for n=2 [59]. Search for large extra dimensions via single photon plus missing energy at D0 sets the limit $M_P^{\rm min}$=0.778 TeV for n=8 to $M_P^{\rm min}$=0.884 TeV for n=2 [60].

The expected limits on string mass scale, black hole mass and string ball mass at ATLAS and CMS detectors are as follows. With an integrated luminosity of $100pb^{-1}$ at proton-proton collisions at $\sqrt{s}$=10 TeV at ATLAS one finds $M_s^{\rm min} \sim 1$ TeV [61]. The lower limit of string mass scale M_s may be very close to 1 TeV when the center of mass energy becomes $\sqrt{s}$=14 TeV. A benchmark point for black hole was produced using the CHARYBIDS event generator [62]. When the luminosity is between fraction of pb^{-1} and a few fb^{-1} the black holes with $M_P \leq 4$ TeV and $2 \leq n \leq 6$ can be observed at the CMS detector [63]. Similarly, only a few pb^{-1} are needed to discover black holes with M_P=1 TeV at ATLAS detector at LHC [64].

Hence from the above current experimental and theoretical constraints we find that the parameter regions found by us give sizable numbers of signal events still viable at LHC.

IV. CONCLUSIONS

We have studied Higgs production and decay from TeV scale string balls and black holes in pp collisions at $\sqrt{s} = 14$ TeV at LHC. We have presented the results of total cross section of diphotons, invariant mass distribution of the diphotons and p_T distribution of the diphotons and ZZ pairs from Higgs from string balls and black holes at LHC. We have found that if string mass scale $M_s \sim$ TeV then the total cross section of diphotons from Higgs from string balls is larger than that from standard model Higgs. The result is more striking for the case of black holes where the total cross section of diphotons from Higgs from black holes is larger than that from standard model Higgs plus background processes. We have found that the invariant mass distribution of the diphotons from Higgs from string balls and black holes is not very sensitive to the increase in diphoton invariant mass. We have also found that $\frac{d\sigma}{dp_T}$ of high p_T diphotons and ZZ pairs produced from Higgs from string balls and black holes is larger than that from standard model Higgs, and also from diphotons and ZZ pairs produced directly from parton fusion processes at LHC. We have observed that $\frac{d\sigma}{dp_T}$ of diphotons and ZZ pairs from Higgs from black holes increases with increase in p_T, whereas from Higgs from string balls it does not decrease sharply with increase in p_T, and from NLO pQCD Higgs it decreases rapidly. Hence the measurement of diphotons and ZZ pairs at LHC can be used to distinguish between Higgs production from: 1) black holes, 2) string balls and 3) parton fusion processes at CERN LHC.

One might wonder if some of the parameters can be extracted. This can be done by obtaining the Planck mass from extra dimensions search at LHC from graviton exchange processes and/or from graviton production processes in partonic collisions [65] at ATLAS and CMS detectors [66–69]. This procedure is not by using string balls and black holes, but is similar to extra dimensions search at LEP [56] and Tevatron [57–60]. Once a value of the Planck mass is obtained from extra dimensions search at ATLAS and CMS detectors [66–69], it can be used to study black holes and string balls at LHC.

In order to look for new physics at LHC by using Higgs from string balls and black holes we may need to address the following questions. Imagine a signal of SB/BH Higgs production will be measured, what would we learn? About the nature of the Higgs? What would not be known before already? Suppose we do not find Higgs from standard model processes at LHC but find it from string balls or black holes, then it may lead to study of Higgs mechanism in string theory [20–23] and quantum gravity [24–27]. If the Higgs is from Higgs mechanism in string theory and/or quantum gravity then it will be associated with the geometrical understanding of the spontaneous symmetry breaking rather than with the electroweak symmetry breaking. The geometrical understanding of spontaneous symmetry breaking in string theory [21] can serve the intuition in the search for realistic models [70, 71]. In gravity, the geometrical understanding of spontaneous symmetry breaking [24] can serve to look for gravitational grand unified theory or GraviGUTs [72]. Hence if we find Higgs from string balls and black holes at LHC then it will provide foundations for many new physics which would not be known before already.

String balls (black holes) might also be produced in PbPb collisions with a larger rate [15]. In this case there can be additional effects of quark-gluon plasma [73] on the string ball (black hole) radiation [31, 44].

Acknowledgments

This work was supported in part by Department of Energy under contracts DE-FG02-91ER40664, DE-FG02-04ER41319 and DE-FG02-04ER41298.

---

[1] N. Arkani-Hamed, S. Dimopoulos and G.R. Dvali, Phys. Lett. **B429**, 263 (1998); Phys. Rev. D**59**,086004 (1999); I. Antoniadis, N. Arkani-Hamed, S. Dimopoulos and G.R. Dvali, Phys. Lett. **B436**, 257 (1998); L. Randall and R. Sundrum, Phys. Rev. Lett. **83**, 3370 (1999); **83**, 4690 (1999).

[2] T. Banks and W. Fischler, hep-th/9906038.

[3] S. Dimopoulos and G. Landsberg, Phys. Rev. Lett. **87**, 161602 (2001); P.C. Argyres, S. Dimopoulos and J. March-Russell, Phys. Lett. **B441**, 96 (1998).

[4] S. B. Giddings and S. Thomas, Phys. Rev. D **65**, 056010 (2002).

[5] S. B. Giddings, in *Proc. of the APS/DPF/DPB Summer Study on the Future of Particle Physics (Snowmass 2001)* ed. R. Davidson and C. Quigg, hep-ph/0110127; M.B. Voloshin,

Phys. Lett. **B518**, 137 (2001); Phys. Lett. **B524**, 376 (2002).

[6] D. M. Eardley and S. B. Giddings, Phys. Rev. D **66**, 044011 (2002); S.N. Solodukhin, Phys. Lett. **B533**, 153 (2002); A. Jevicki and J. Thaler, Phys. Rev. D**66**, 024041 (2002).

[7] L. Anchordoqui and H. Goldberg, Phys. Rev. D **65**, 047502 (2002); Phys. Rev. D**67**, 064010 (2003).

[8] R. Casadio and B. Harms, Int. J. Mod. Phys. A **17**, 4635 (2002).

[9] K. Cheung, Phys. Rev. D **66**, 036007 (2002); Phys. Rev. Lett. **88**, 221602 (2002); K. Cheung and Chung-Hsien Chou, Phys. Rev. D **66**, 036008 (2002); G. C. Nayak, hep-ph/0211395; arXiv:0901.3358 [hep-ph].

[10] Y. Uehara, Mod. Phys. Lett. A **17**, 1551 (2002).

[11] Seong Chan Park and H.S. Song, J. Korean Phys. Soc. **43**, 30 (2003).

[12] M. Bleicher, S. Hofmann, S. Hossenfelder and H. Stoecker, Phys. Lett. B **548**, 73 (2002); S. Hossenfelder, S. Hofmann, M. Bleicher and H. Stoecker, Phys. Rev. D **66**, 101502 (2002).

[13] I. Mocioiu, Y. Nara and I. Sarcevic, Phys. Lett. B**557**, 87 (2003); V. Frolov and D. Stojkovic, Phys. Rev. D **68**, 064011 (2003); **67**, 084004 (2003); **66**, 084002 (2002); D. Ida and S. C. Park, Phys. Rev. D **67**, 064024 (2003); **69**, 049901 (E) (2004); B. Kol, hep-ph/0207037; M. Cavaglia, S. Das and R. Maartens, Class. Quant. Grav. **20**, 1205 (2003); M. Cavaglia and S. Das, Class. Quant. Grav. **21**, 4511 (2004); S. Hosenfelder, Phys. Lett. **B598**, 92 (2004); A. Ringwald, Fortsch. Phys. **51**, 830 (2003).

[14] T. Han, G. D. Kribs and B. McElrath, Phys. Rev. Lett. **90**, 031601 (2003).

[15] A. Chamblin and G. C. Nayak, Phys. Rev. D66 (2002) 091901.

[16] A. Chamblin, F. Cooper and G. C. Nayak, Phys. Lett. B672 (2009) 147; Phys. Rev. D70 (2004) 075018; Phys. Rev. D69 (2004) 065010.

[17] L. A. Anchordoqui, J. L. Feng, H. Goldberg and A. D. Shapere, Phys. Rev. D **66**, 103002 (2002); J. L. Feng and A. D. Shapere, Phys. Rev. Lett. **88**, 021303 (2002); L. A. Anchordoqui, T. Paul, S. Reucroft and J. Swain, Int. J. Mod. Phys. A **18**, 2229 (2003).

[18] R. Emparan, M. Masip and R. Rattazzi, Phys. Rev. D **65**, 064023 (2002).

[19] A. Ringwald and H. Tu, Phys. Lett. B **525**, 135 (2002).

[20] J. Bagger and I. Giannakis, Phys.Rev. D56 (1997) 2317, hep-th/9703202.

[21] S. Foerste, H. P. Nilles and A. Wingerter, Phys.Rev. D73 (2006) 066011, hep-th/0512270.

[22] S. Watson, Phys.Rev. D70 (2004) 066005, hep-th/0404177.

[23] F. Aldabe, hep-th/9506168.

[24] R. Percacci, Nucl. Phys. B353, 271-290 (1991), arXiv:0712.3545 [hep-th].

[25] I. Kirsch, Phys.Rev. D72 (2005) 024001, hep-th/0503024.

[26] I. Kirsch, Phys.Rev. D72 (2005) 024001, hep-th/0503024.

[27] S. Mukohyama, JHEP0705:048,2007, hep-th/0610254.

[28] L. Susskind, hep-th/9309145.

[29] M. J. Bowick, L. Smolin and L. C. Wijewardhana, Phys. Rev. Lett. 56 (1986) 424; E. Halyo, B. Kol, A. Rajaraman and L. Susskind, Phys. Lett. B 401 (1997) 15; G. Veneziano, in *NATO Advanced Study Workshop on Hot Hadronic Matter: Theory and Experiment,* Divonne-les-Bains, France, 27 Jun-1 jul 1994; G. T. Horowitz and J. Polchinski, Phys. Rev. D55 (1997) 6189; Phys. Rev. D57 (1998) 2557; T. Damour G. Veneziano, Nucl. Phys. B568 (2000) 93.

[30] S. Dimopoulos and R. Emparan, Phys. Lett. B526 (2002) 393, hep-ph/0108060.

[31] D. Amati and J. G. Russo, Phys. Lett. B454 (1999) 207, hep-th/9901092.

[32] D. M. Gingrich and K. Martell, Phys. Rev. D78 (2008) 115009, arXiv:0808.2512 [hep-ph].

[33] D. de Florian and M. Grazzini, Phys.Lett.B674:291-294,2009; R. Harlander, J.Phys.G35:033001,2008; M. Ciccolini, A. Denner and S. Dittmaier, Phys.Rev.D77:013002,2008; G. Bozzi, S. Catani, D. de Florian, Nucl.Phys.B791:1-19,2008; G. Klamke, D. Zeppenfeld, JHEP 0704:052,2007; S. Catani, M. Grazzini, Phys.Rev.Lett.98:222002,2007; E. Gabrielli, F. Maltoni, B. Mele, M. Moretti, F. Piccinini and R. Pittau, Nucl.Phys.B781:64-84,2007; T. Hahn, S. Heinemeyer, F. Maltoni, G. Weiglein and S. Willenbrock, e-Print: hep-ph/0607308; D. Graudenz, M. Spira and P. Zerwas, Phys. Rev. Lett. **70**, 1372 (1993); G. Bozzi, S. Catani, D. de Florian and M. Grazzini, Phys.Lett.B564:65-72,2003; V. A. Khoze, Alan D. Martin and M.G. Ryskin, Eur.Phys.J.C21:99-103,2001; Z. Kunszt, S. Moretti and W.James Stirling, Z.Phys.C74:479-491,1997; M. Spira, A. Djouadi, D. Graudenz and P. Zerwas, Phys. Lett. **B318**, 347 (1993); Nucl. Phys. **B453**, 17 (1995); M. Krämer, E. Laenen and M. Spira, Nucl. Phys. **B511**, 523 (1998); V. Ravindran, J. Smith and W.L. van Neerven, Nucl. Phys. **B704**, 332 (2005); R.V. Harlander and W.B. Kilgore, Phys. Rev. Lett. **88**, 201801 (2002); C. Anastasiou and K. Melnikov, Nucl. Phys. **B646**, 220 (2002).

[34] V. Ravindran, J. Smith and W. L. van Neerven, Nucl. Phys. **B665**, 325 (2003).

[35] V. Ravindran, J. Smith and W. L. van Neerven, Nucl. Phys. **B634**, 247 (2002).

[36] G. Landsberg, Phys. Rev. Lett. 88 (2002) 181801.

[37] Y. Uehara, hep-ph/0205122.

[38] G. C. Nayak and J. Smith, Phys. Rev. D **74**, 014007 (2006), *Haunting Higgs Boson in Mini Black Holes*, issue 2562, New Scientist, 28 July 2006, p12.

[39] A. E. Erkoca, G. C. Nayak and I. Sarcevic, Phys. Rev. D79 (2009) 094011.

[40] K. Prokofiev, The ATLAS collaboration, ATL-PHYS-PROC-2009-008.

[41] D. Trocino, The CMS collaboration, CMS CR-2008/108.

[42] A. Drozdetskiy, The CMS collaboration, CMS CR-2007/038.

[43] C. M. Harris and P. Kanti, JHEP 0310, 014 (2003); N. Sanchez, Phys. Rev. D16, 937 (1977); Phys. Rev. D18, 1030 (1978); Phys. Rev. D18, 1798 (1978).

[44] R. Emparan, G. T. Horowitz and R. C. Myers, Phys. Rev. Lett. **85**, 499 (2000).

[45] G. C. Nayak, JHEP06(2009)071.

[46] J. Pumplin et al., JHEP **0207**, 102 (2002).

[47] B. Lenzi, arXiv:0808.0162 [hep-ex].

[48] *Expected Performance of the ATLAS Experiment - Detector, Trigger and Physics*, The ATLAS Collaboration, G. Aad *et al.*, e-Print: arXiv:0901.0512 [hep-ex].

[49] *Prospects for the Discovery of the Standard Model Higgs Boson Using the $H \to \gamma\gamma$ Decay*, The ATLAS collaboration, ATL-PHYS-PUB-2009-053.

[50] *Prospects for the Higgs Searches with the ATLAS detector*, Acta Phys.Polon.B40:1909-1930,2009, arXiv:0903.4198 [hep-ex].

[51] C. Aurenche and C. Seez, *in Proc. Large Hadron Collider Workshop*, Aachen, edited by G. Jarlskog and D. Rein, CERN 90-10/ECFA 90-133 (1990).

[52] M. Gataullin, The CMS collaboration, arXiv:0810.3753 [hep-ex].

[53] E. L. Berger and J. Campbell, Phys. Rev. D70 (2004) 073011.

[54] V. Del Duca, F. Maltoni, Z. Nagy and Z. Trocsanyi, JHEP0304(2003)059.

[55] G. Sanguinetti and S. Karg, arXiv:0806.1394 [hep-ph].

[56] J. Abdallah *et al.*, DELPHI Collaboration, Eur.Phys.J.C60:17-23,2009, arXiv:0901.4486 [hep-ex].

[57] A. Abulencia *et al.*, The CDF Collaboration, Phys.Rev.Lett.97:171802,2006, hep-ex/0605101.

[58] T. Aaltonen *et al.*, The CDF Collaboration, Phys. Rev. Lett. 101, 181602 (2008), arXiv:0807.3132.

[59] V.M. Abazov *et al.*, The D0 Collaboration, Phys.Rev.Lett.102:051601,2009, arXiv:0809.2813

[hep-ex].

[60] V.M. Abazov *et al.*, The D0 Collaboration, Phys.Rev.Lett.101:011601,2008, arXiv:0803.2137 [hep-ex].

[61] *Search for highly-excited string states with ATLAS*, D. M. Gingrich, The ATLAS Collaboration, ATL-PHYS-PUB-2009-011.

[62] C. M. Harris *et al.*, JHEP 08 (2003) 033, hep-ph/0307305.

[63] *Search for monojets and black holes at CMS*, L. Sala, The CMS collaboration, CMS CR-2009/003.

[64] *Discovery reach for miniblack holes with the ATLAS detector at the LHC*, M. Kaneda, The ATLAS collaboration, ATL-PHYS-PROC-2009-024.

[65] G. F. Giudice, R. Rattazzi and J. D. Wells, Nucl.Phys.B544:3-38,1999, hep-ph/9811291.

[66] *Search for extra dimensions with the CMS detector*, S. Shmatov, The CMS Collaboration, Nucl.Phys.Proc.Suppl.177-178:330-332,2008.

[67] *Search for Extra Dimensions with Atlas and CMS Detectors at the LHC.*, S. Shmatov, arXiv:0707.0470 [hep-ex].

[68] *Search for extra dimensions and compositeness at CMS*, G. Kim, The CMS Collaboration, AIP Conf.Proc.1078:623-625,2009.

[69] *Probing Extra Dimensions with ATLAS*, D. Dannheim, AIP Conf.Proc.903:261-264,2007, hep-ex/0611005.

[70] L. J. Dixon, J. A. Harvey, C. Vafa and E. Witten, Nucl. Phys. B261 (1985) 678.

[71] L. J. Dixon, J. A. Harvey, C. Vafa and E. Witten, Nucl. Phys. B274 (1985) 285.

[72] R. Percacci, arXiv:0910.5167 [hep-th].

[73] F. Cooper, E. Mottola and G. C. Nayak, Phys. Lett. B555, 181 (2003); G. C. Nayak *et al.*, Nucl. Phys. A687, 457 (2001).